OPTICAL PROPERTIES OF DEFORMATION INDUCED DEFECTS IN MgO SINGLE CRYSTALS

By

RICKY DAN NEWTON

Bachelor of Science

East Central Oklahoma State University

Ada, Oklahoma

1974

Submitted to the Faculty of the Graduate College
of the Oklahoma State University
in partial fulfillment of the requirements
for the Degree of
MASTER OF SCIENCE
December, 1976

OPTICAL PROPERTIES OF DEFORMATION INDUCED

DEFECTS IN MgO SINGLE CRYSTALS

Thesis Approved:

W. A. Sibley

Thesis Adviser

Joel J. Martin

Richard C. Powell

Norman N. Durham

Dean of the Graduate College

ACKNOWLEDGEMENTS

The author wishes to express his appreciation to his major advisor, Dr. W. A. Sibley, for suggesting this problem and for his guidance and assistance throughout this study. Appreciation is also extended to Dr. S. I. Yun for his assistance with the thermoluminescence study.

The author gratefully acknowledges the financial support provided by the National Science Foundation and the Department of Physics at Oklahoma State University.

Finally, I wish to express special thanks to my father for his many sacrifices and continuing support.

TABLE OF CONTENTS

LIST OF TABLE

LIST OF FIGURES

CHAPTER I

INTRODUCTION

In the field of solid state physics, the study of defects in crystalline solids is of great interest because of their importance in device and structural physics. By studying a crystal which contains imperfections, much can be learned about the perfect crystal lattice. In many cases, defects in a solid are responsible for properties which make the material useful in electronic devices. If the material is considered for use as a structural material, it is particularly important to learn how the defects that may be created by stresses or proximity to radiation sources will affect the properties of material, such as hardness, radiation damage sensitivity, or electrical conductivity.

Some types of defects can be produced simply by deforming crystals by bending, indenting, or compressing. If a crystal is subjected to a force along one crystallographic axis the crystal will yield plastically by a process called glide (1). Glide is a translation of one part of the crystal with respect to another part. In a cubic crystal, glide usually takes place on one or more crystallographic planes, called slip planes, and in one particular direction. However, not all atoms above the slip plane move simultaneously to their new positions with respect to the atoms below the slip plane. The result is that the displacement of the upper block of crystal relative to the lower block varies from region to region within the crystal. Lines in the slip plane separating

regions where slip has occurred from regions where it has not are called dislocations (1).

If one continues to apply stress to the crystal, the dislocations will begin to move through the crystal lattice, leaving behind debris when they encounter impurity atoms or other dislocations. Seitz, in 1952, proposed that these dislocation interactions could generate vacancies and interstitial defects (2). A vacancy is produced by removing an atom from an atomic site, while an interstitial defect is formed by introducing an atom into a non-atomic site within the lattice. Seitz's proposal has since been verified by various researchers (3). Understanding the effect of these deformation-induced defects is very important. In some cases, it is possible to observe the effects of the dislocations directly. The emerging points of dislocations can sometimes be observed by etching the surface of the crystal with a suitable chemical (4,5,6). In this way one can study the motion of the dislocations and their arrangement in the deformed crystal. If the crystal under study is transparent to light or infra-red radiation, it is possible to decorate the dislocations, which are normally invisible, by inducing precipitation along the dislocation line (4,7). This technique usually involves heating the crystal, which causes "beads" or precipitates to form at the dislocation sites. The dislocations can then be observed with a light microscope.

A great deal has been learned about dislocations and their interactions by electron microscope studies (4,8). This technique is potentially applicable to any material which can be produced in very thin sections. The maximum resolution of the electron microscope is about 4A, which usually does not permit the examination of the atomic arrange-

ment around the dislocation. X-ray diffraction techniques are similar to those of electron microscopy, but the resolution is greatly reduced (4). The advantage of X-rays over electrons is that X-rays penetrate much farther than electrons so that thicker samples may be examined. The maximum resolution currently available is 2-3A obtained by the field ion microscope (9).

Indirect observations can tell one a great deal about the type of defects present in a crystal. These techniques include electron spin resonance (10,11) and optical methods, about which we shall speak in detail later.

The alkaline-earth oxides such as SrO, CaO and MgO are particularly well-suited as subjects for dislocation interaction studies, and they have been studied extensively in recent years. These materials are relatively resistant to defect formation except by forceful means, such as irradiation with energetic particles or deformation (12). MgO is the only alkaline-earth oxide which is non-hygroscopic. This property, together with its hardness, make MgO attractive for use as a structural material. MgO has been suggested for use as one of the insulating materials in the proposed Theta Pinch nuclear fusion reactor (13). MgO is also used in electronic components where a high temperature dielectric is needed. Because MgO might be used in an application which would subject it to stress or high temperature, it is necessary to know how the properties of MgO would be affected by these conditions.

Dislocations and dislocation interactions in MgO have been studied directly by etch pit and decoration techniques (14) and by electron microscopy (15,16). Electron spin resonance studies have yielded much information about the type of defects formed by deformation in MgO

(17,18,19).

Since MgO is transparent over a wide range of wavelengths, optical methods of investigation can provide insight into the effect of the deformation-induced defects. Previous researchers have studied the absorption (19,20,21), the luminescence (12,19,22), and the thermoluminescence (19,23) in deformed MgO.

In this study we will use the optical techniques of absorption, luminescence, and thermoluminescence to study the effects of defects produced by deforming MgO by compression. We will attempt to correlate the luminescence with the absorption and excitation spectra and to determine the relationship between the degree of absorption and amount of deformation and the intensity of emission and amount of deformation. We will also investigate the effect of the shape of the sample on its deformation induced absorption. By deforming and optically measuring samples which have various length to thickness ratios we will determine if there is a sample shape factor which has an effect on the concentration of defects produced by deformation.

CHAPTER II

THEORY

In the introduction we discussed briefly how dislocations were formed. We will now discuss more fully the production of dislocations and the subsequent creation of defects by dislocation interactions.

Most crystals deform plastically by means of translational slip, or glide, which means one block of crystal slides as a unit across an adjacent block (4). The crystal plane on which slip takes place is the slip plane. The slip plane, together with the direction of slip, constitute a slip system. Slip is anisotropic; some directions and planes are preferred. The slip direction is almost always along that direction in which the atoms are most closely packed. In face-centered cubic crystals, such as MgO, slip takes place in <110> directions on {110} planes.

Slip takes place when the shear stress along a certain slip direction reaches a critical value. If a force F is applied to a crystal with surface area A along a <100> axis, the applied stress will be F/A. The shear stress τ resolved in the slip direction is

$$\tau = (F/A) \cos\phi \cos\lambda \qquad (1)$$

where ϕ and λ are the angles the direction of force makes with the normal to the slip plane and the slip direction respectively (24). If F_c is the force required to produce slip, then τ_c is the critical resolved

shear stress. In crystals, such as MgO, which slip in <110> directions $\phi = \lambda = \frac{\pi}{4}$. Hence the critical resolved shear stress is

$$\tau_c = \tau/2 = F/(2A). \tag{2}$$

The theoretical value of the critical resolved shear stress was first calculated by Frenkel (25). He considered the simple case of the shearing of two rows of atoms past each other in a homogeneous crystal. Frenkel let the spacing between the rows be a, the spacing between the atoms in the row be b, and the displacement of one row relative to the other be x. He then proposed the shear stress to be

$$\tau = (Gb)/(2\pi a) \sin (2\pi x/b) \tag{3}$$

where G is the shear modulus. Since the shear force must be zero when the row of atoms moves into a normal lattice site and also halfway between normal lattice sites, the force must be a periodic function of displacement. The theoretical value for the critical shear stress would then be the maximum value of τ,

$$\tau_{th} = (Gb)/(2\pi a) \tag{4}$$

Since $b \approx a$, τ_{th} is approximately $G/2\pi$. This value of τ_{th} is several orders of magnitude greater than the actual critical shear stress observed in real crystals.

More recent calculations of τ_{th} have taken into account two factors not considered by Frenkel (24). One is the hardness factor, which is the steepness with which the repulsive force between atoms builds up as atoms are brought together. The critical strain which must be ex-

ceeded to break the bond between atoms is smaller for "hard" atoms than for "soft" ones. The second factor takes into account the possible configurations of mechanical stability, such as twinning, through which the lattice may pass as it is sheared. This means that the sinusoidal relation of Eq. 3 may oscillate over periods smaller than the lattice spacing, thus reducing the shear strength. Mackenzie took these two factors into account and showed that the minimum value of the theoretical shear strength is G/30 (26). This value is still much larger than the observed strength of real crystals.

The error in these calculations is in assuming that one block of atoms moves as a unit across an adjacent block when a stress is applied to the crystal. Actually, the process of plastic deformation consists of slips which do not take place simultaneously in the whole glide plane. Hence the glide plane contains slipped and unslipped areas. The boundary between slipped and unslipped areas is a line defect or dislocation. The dislocation may be either a closed loop or a half loop extending from surface to surface which sweeps along the glide plane during deformation. It is the creation and movement of dislocations which accounts for the low shear strength of real crystals (27,28).

There are two basic types of line dislocations, edge and screw dislocations. These are illustrated in Figure 1. An edge dislocation has, in effect, an extra half-plane of atoms inserted into the lattice. A positive edge dislocation has the extra half-plane of atoms inserted above the slip plane, while a negative edge dislocation has the extra half-plane of atoms inserted below the slip plane. The Burgers vector of an edge dislocation is normal to the line of the dislocation. A screw dislocation can be geometrically described as a single-surface

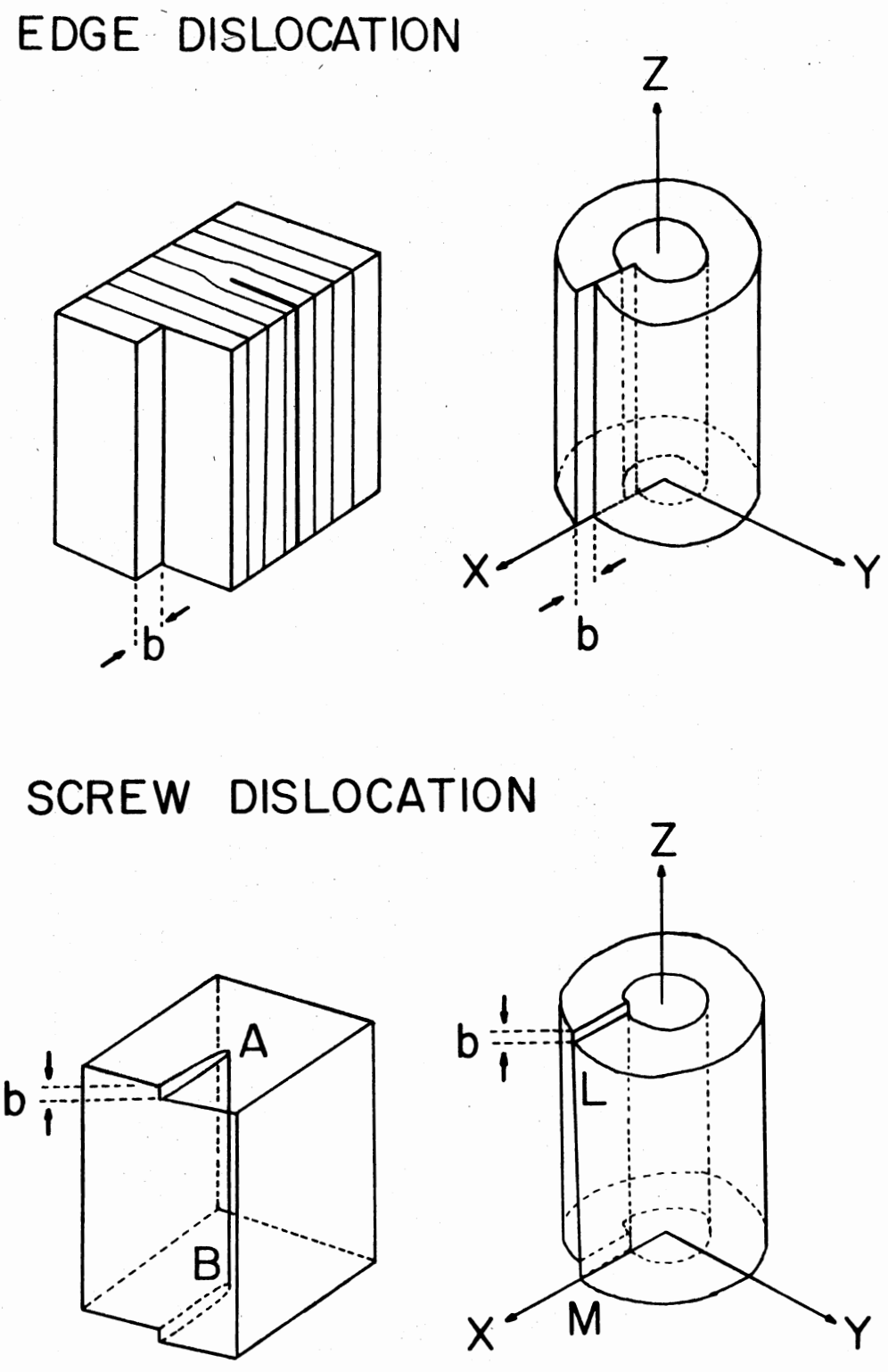

Figure 1. Edge and Screw Dislocations in Crystals

helicoid. A screw dislocation may be either right-handed or left-handed depending on whether the helix advances or retreats one plane when a clockwise circuit is made around the dislocation line. The Burgers vector of a screw dislocation is parallel to the line of the dislocation.

The number of dislocations per unit volume of a crystal is the dislocation density, N, defined as the total length of dislocations per unit volume, usually in units of cm^{-2}. N is usually lower in non-metallic crystals than in metals. A typical value of dislocation density in MgO is 2×10^{9} cm^{-2} in a single crystal compressed 9% at a deformation rate of 2×10^{-3} cm/sec (18). It has been shown that the dislocation densities in slip bands in ionic crystals increase progressively with increasing applied shear stress (29). In face centered cubic crystals the dislocation density is approximately proportional to the strain so that

$$N \approx 10^{9} \varepsilon \ cm^{-2} \tag{5}$$

for strains of 0.1% to 10% (30).

When a crystal is subjected to an applied force, a dislocation in it will move in the direction that offers least resistance. A dislocation is highly mobile in the sense that a small applied stress can overcome the resistance of the lattice. The stress necessary to move the dislocation is several orders of magnitude smaller than the shear modulus. The high mobility of the dislocation is necessary to explain the low shear strength, since the yield stress of ionic crystals is determined primarily by the stress required to move dislocations in them.

There are two basic types of dislocation movement, glide or conser-

vative motion in which the dislocation moves in the surface defined by its line and Burgers vector, and climb or non-conservative motion in which the dislocation moves out of the glide surface. Non-conservative motion leads to the creation of defects, because as the dislocation moves through the lattice, it leaves voids or excesses of matter, so the total volume of the crystal is not conserved.

As plastic deformation proceeds, slip will occur on other slip systems and the dislocations on one slip plane will intersect dislocations on another slip plane. The intersection of dislocations creates jogs which are steps in the original dislocations. As the jogs themselves move non-conservatively through the lattice, they leave behind a trail of vacancies or interstitial atoms (24). Whether vacancies or interstitials will be generated by the movement of the jog depends on the sign of the dislocation and the direction the dislocation is moving. Under certain circumstances, a jog can leave a trail of two edge dislocations with the same Burgers vector but of opposite sign. This is called a dislocation dipole (27).

The production of the dislocations and their interactions contribute to another phenomenon of plastic deformation. The dislocations introduced by strain contribute to the strength of the crystal due to the mutual interaction between dislocations. Crystals harden progressively as straining proceeds, and the process is called work hardening or strain hardening (4). Hardening can be caused by substitutional atoms in the crystal lattice or by vacancies and interstitial atoms (31). The electrostatic interaction between dislocations and point defects also contributes to hardening (32). Another important cause of strain hardening is the debris left in the wake of moving screw dislo-

cations (33). The debris consists of edge dislocation dipoles which inhibit the motion of subsequent dislocations on the same or nearby glide planes, and thereby increase the flow stress (34). Dislocation dipoles are created when multiple cross-slip occurs. Cross slip is said to occur when a dislocation leaves one close packed plane for another intersecting close packed plane (24).

CHAPTER III

EXPERIMENTAL PROCEDURE

The MgO crystals used in this study were cleaved from ingot OR-18 obtained from the Oak Ridge National Laboratory. A chemical analysis of the MgO samples used has been performed. A table of impurities is presented in Table I. The samples, which were of various sizes, were compressed along <100> directions in an Instron testing machine with a crosshead speed of S_c = 0.05 cm/min. The stress applied to the sample was recorded on a strip chart which moved at a rate of 5.0 cm/min.

When compressing a crystal, part of the crosshead motion goes into the elastic strain of the Instron (35). This "softness" of the Instron can be depicted by an imaginary spring. The elastic displacement due to the softness of the Instron is $\Delta y_{el} = F/K$, where F is the applied force and K is the effective spring constant. If ΔL_p is the amount of plastic deformation of the crystal, the total crosshead displacement is

$$\Delta y = S_c t = \Delta y_{el} + \Delta L_p \qquad (6)$$

where t is the time, determined by the displacment of the chart divided by the chart speed. The plastic strain is

$$\varepsilon = (\Delta L_p/L_0) = (S_c t - F/K)/L_0, \qquad (7)$$

where L_0 is the original length of the crystal. The plastic strain rate

TABLE I

CHEMICAL ANALYSIS OF MgO SINGLE CRYSTAL SERIAL NO. OR-18 FROM OAK RIDGE NATIONAL LABORATORY

Impurity	μ g/g	Impurity	μ g/g
Ag	< 1	Mo	< 1
Al	62	Na	< 0.5
As	5	N	< 1
B	< 2	Ni	< 3
Ba	< 2	P	< 1
Be	< 1	Pb	< 0.5
Bi	< 3	Rb	< 5
Ca	36	S	< 2
Co	< 5	Sb	< 5
Cr	1	Si	10
Cu	~< 1 (Trace)	Sn	< 3
Fe	3-7	Ti	3
K	< 5	V	< 5
Li	< 1	Zn	< 0.5
Mn	1.0	Zr	2

is the time derivative of the strain,

$$\dot{\varepsilon} = d\varepsilon/dt = (S_c - K^{-1} dF/dt)/L_0. \quad (8)$$

Values of Δy_{el} for the Instron used in this study were determined by compressing a piece of relatively incompressible stainless steel between the platens of the machine. Strain was then computed using Eq. 7.

Optical absorption measurements were made using a Cary Model 14 spectrophotometer, which records the optical density of the sample as a function of wavelength. Optical density is $\log_{10}(I/I_0)$ where I_0 and I are the intensities of the sample and reference beams respectively. Determination of the absorption coefficient was made using the expression

$$\alpha = (O.D.) \times 2.303/t \text{ cm}^{-1} \quad (9)$$

where t is the thickness of the sample in cm. The thickness was measured using a micrometer. The optical density (O.D.) was obtained by subtracting the optical density of the deformed sample from the optical density of the as-cleaved sample at some particular wavelength.

Luminescence emission measurements were made using the apparatus shown in Figure 2. The excitation source was a PEK Industries 100W short arc Hg lamp, 75W short arc Xe-Hg lamp, or 150W short arc Xe lamp. Exciting light was chopped with a light chopper at a frequency of 135 Hz before passing through a Spex Industries, Inc. 22 cm. Minimate monochromator. The light was focused by lenses and reflected by a front surface mirror onto the front surface or the edge of the sample. The luminescence was analyzed by a Jarrel-Ash one-meter Czerny-Turner

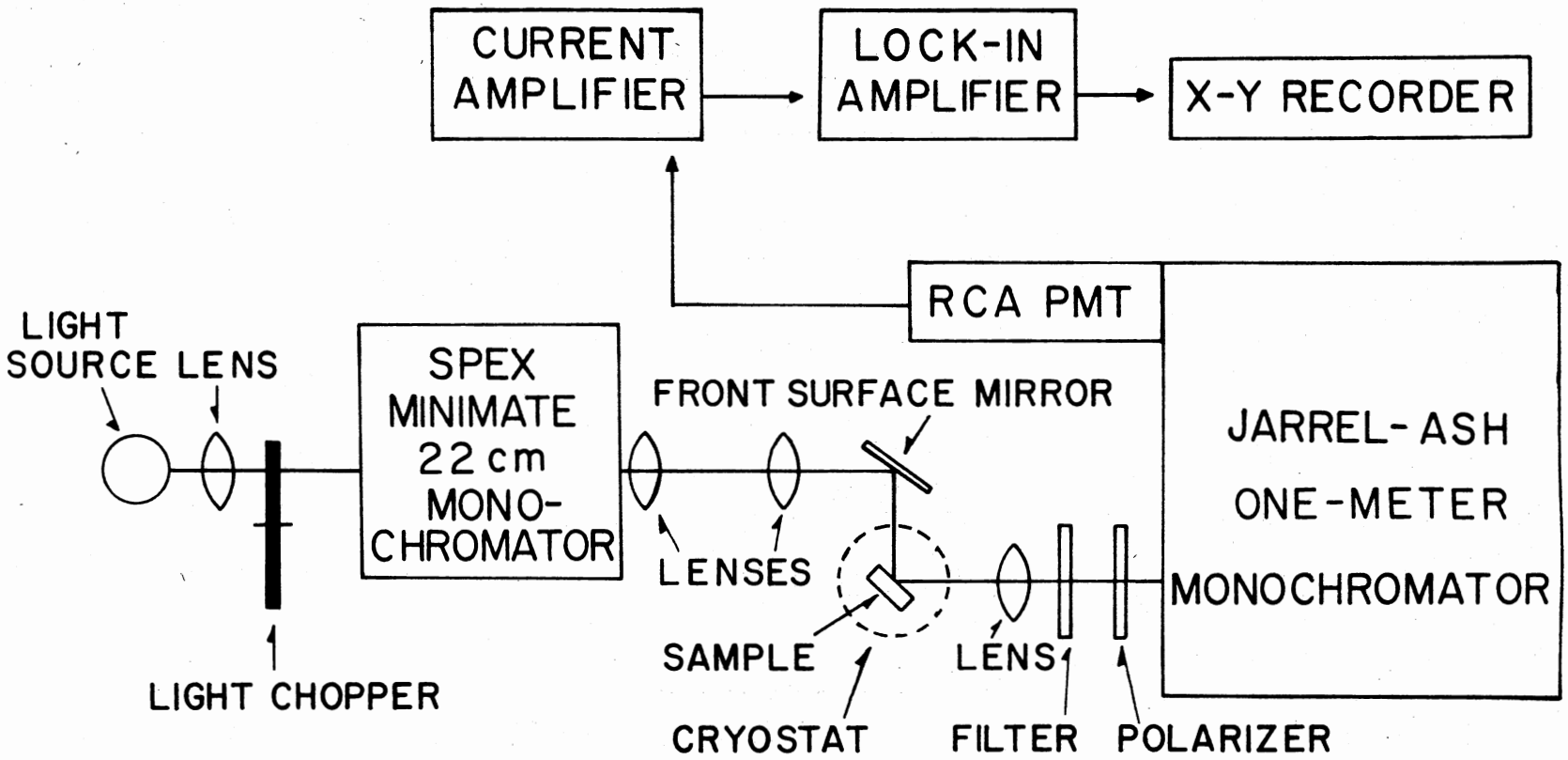

Figure 2. Block Diagram of Luminescence Apparatus

monochromator having a dispersion of 8.2 A/mm. The luminescence was detected by a RCA C31034 photomultiplier tube operated at 1800 VDC. The photomultiplier was cooled to -27°C by a Products for Research, Inc., Model TE-104 thermoelectric cooler. The output of the photomultiplier tube was amplified by a Keithley Model 427 current amplifier and a Keithley Model 840 lock-in amplifier. The spectrum was displayed on a Mosley Model 7000A or Houston Model 2000 X-Y recorder.

The optical excitation spectrum was taken using the same apparatus. Exciting light from the 150W Xe lamp passed through the Spex Minimate monochromator which was driven by a synchronous motor drive. The Jarrel-Ash monochromator was set to the peak of the luminescence band and then the Spex monochromator was scanned from 200 nm to about 310 nm. Corning glass filters which sharply cut off wavelengths below 300 nm were used to decrease the effect of higher order exciting light being detected by the phototube. The intensity of 440 nm emission was displayed as a function of wavelength of exciting light on an X-Y recorder.

For low temperature measurements of absorption or emission the sample was mounted in a Sulfurine liquid helium cryostat or in a Cryogenic Technology, Inc. Model 20/70 Cryodyne cryogenerator. When mounted in the Sulfurine cryostat, the sample could be cooled to 77K using liquid nitrogen or to 4K using liquid helium. In the cryogenerator, the temperature of the sample could be maintained between 10K and room temperature by balancing the heat input from an internal resistance heater with the heat removed by the cryogenerator.

Thermoluminescence measurements were made by mounting the sample on a brass block in which a resistance heater was imbedded. The voltage to the heater was varied by driving a Variac variable AC power

supply with a synchronous motor drive. Thus the temperature of the sample was increased slowly at an average rate of approximately 2^{o}C/min. An EMI 9558Q phototube operated at 700 VDC at room temperature viewed one edge of the sample through a light pipe. Current from the EMI phototube was amplified by a Keithley Model 427 current amplifier and the signal was displayed on the y-axis of an X-Y recorder. An Iron-Constantan thermocouple provided a temperature-dependent voltage which drove the x-axis of the X-Y recorder. Thus the glow curve of thermoluminescence as a function of temperature was obtained.

A spectrum of the thermoluminescence was obtained periodically by scanning the Jarrel-Ash monochromator from 300 to 800 nm. Emitted light was detected by the RCA C31034 photomultiplier tube and the signal amplified by a Keithley Model 427 current amplifier. The spectrum was displayed on a Houston X-Y recorder.

Irradiations were carried out by placing the sample in a Cobalt 60 Gammacell, Model 200, manufactured by Atomic Energy of Canada, Limited.

CHAPTER IV

PRESENTATION AND DISCUSSION OF RESULTS

Stress vs. strain curves for MgO samples with three different length to thickness ratios are shown in Figure 3. One can see that the shape of the sample has an effect in the work hardening region. The slope of the curve is greater for short, thick samples than for long, thin ones. This effect is probably due to the number of slip systems operating. Long, thin samples are more likely to deform by single slip processes, while short, thick samples are likely to have multiple cross slip occurring during deformation. Cross slip would lead to the production of dislocation dipoles, the interaction of which would increase the flow stress. Cross slip and single slip can be observed directly by examining the deformed samples between crossed polarizers.

The principle absorption band in deformed MgO occurs at 5.7 eV (215 nm) (19,21). Figure 4 shows the absorption coefficient at 215 nm as a function of per cent deformation. The data points shown are averages of several data points within a region. On the average, data from five samples contributed to each data point shown. The error was computed by

$$\text{error} = \pm d_{max}/\sqrt{n} \tag{10}$$

where d_{max} is the maximum deviation from the average value of α_{215} within the region, and n is the number of data points in the region.

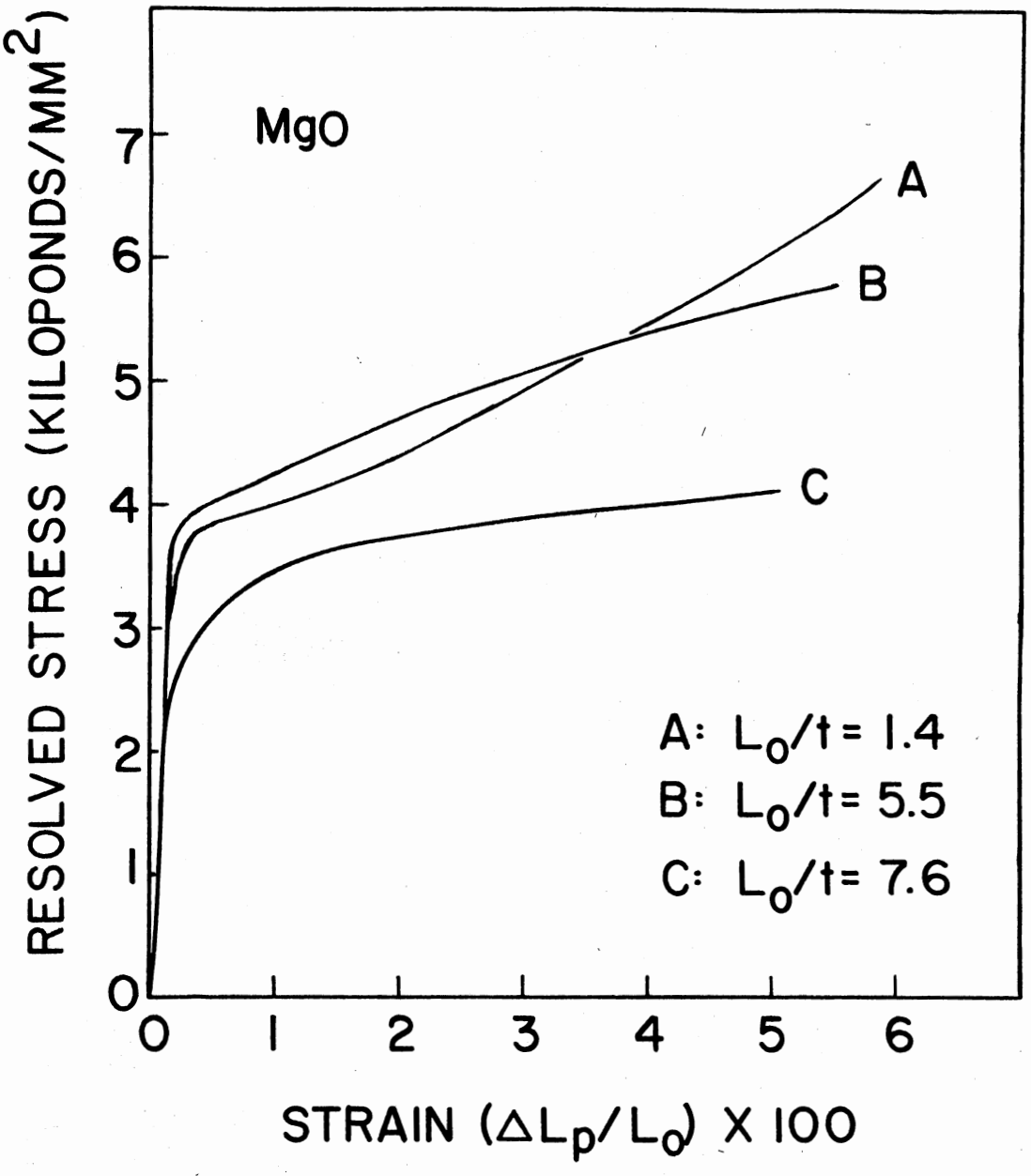

Figure 3. Stress vs. Strain Curves for MgO Samples With Various Length to Thickness Ratios

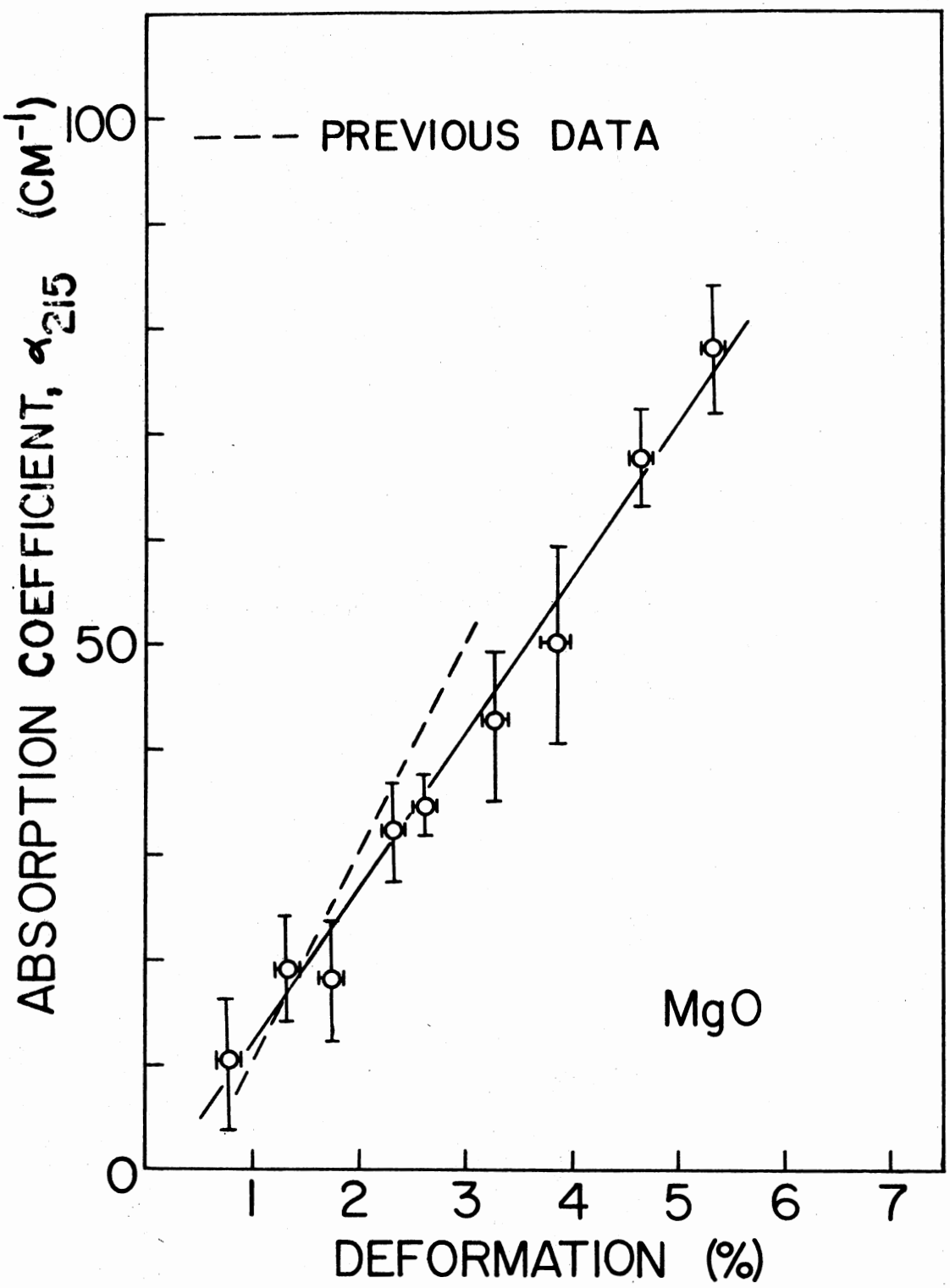

Figure 4. Absorption Coefficient, α_{215}, as a Function of % Deformation in MgO. Results from a previous study by Sibley, et al. (19) are shown for purpose of comparison

Average values were used because scatter made it difficult to draw a best fit curve through the data points. The curve drawn is in close agreement with data presented by Sibley et al. (19). The curve shows the the absorption at 215 nm is a linear function of the strain. This agrees with Gilman and Johnson's finding that dislocation densities in slip bands increase linearly with strain (30).

Since there appeared to be a relation between the shape of the sample and its absorption, a plot of absorption coefficient, α_{215}, divided by per cent deformation as a function of length to thickness ratio was made (Figure 5). The data points and the error bars were determined statistically in the same manner as was done for Figure 4. We see that the slopes of the α_{215} vs. per cent deformation curves would be approximately the same for samples with length to thickness ratios of 5 to 12. However, for samples with L_0/t less than five, the absorption is much reduced. If the 215 nm absorption band is due to vacancy pairs as has been suggested (20), then this result is reasonable, because vacancy pairs are more likely to be produced during the single slip processes occurring during the deformation of long, thin samples. However, the cross slip which occurs during deformation of short, thick samples is more likely to produce vacancy clusters, which have a different absorption.

Absorption spectra at three temperatures for deformed MgO are shown in Figure 6. The sample used for these spectra had a length to thickness ratio of 4.3 and was deformed 1.2%. It is possible to fit the band at 5.7 eV with a Gaussian bandshape, however, there appear to be one or two smaller bands between 4 and 5.2 eV which are more difficult to fit.

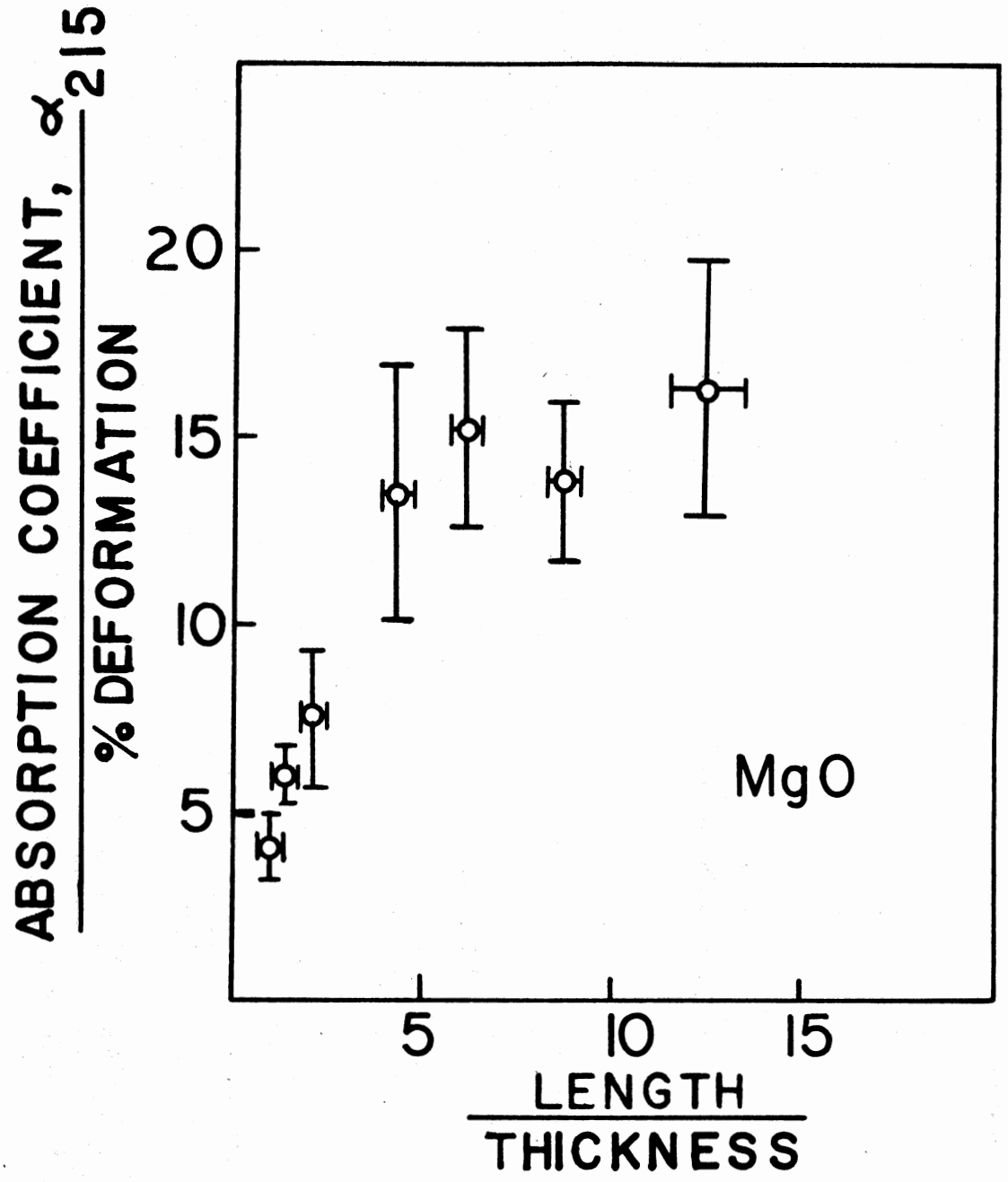

Figure 5. Absorption Coefficient, α_{215}, Divided by % Deformation as a Function of Length to Thickness Ratio in Deformed MgO

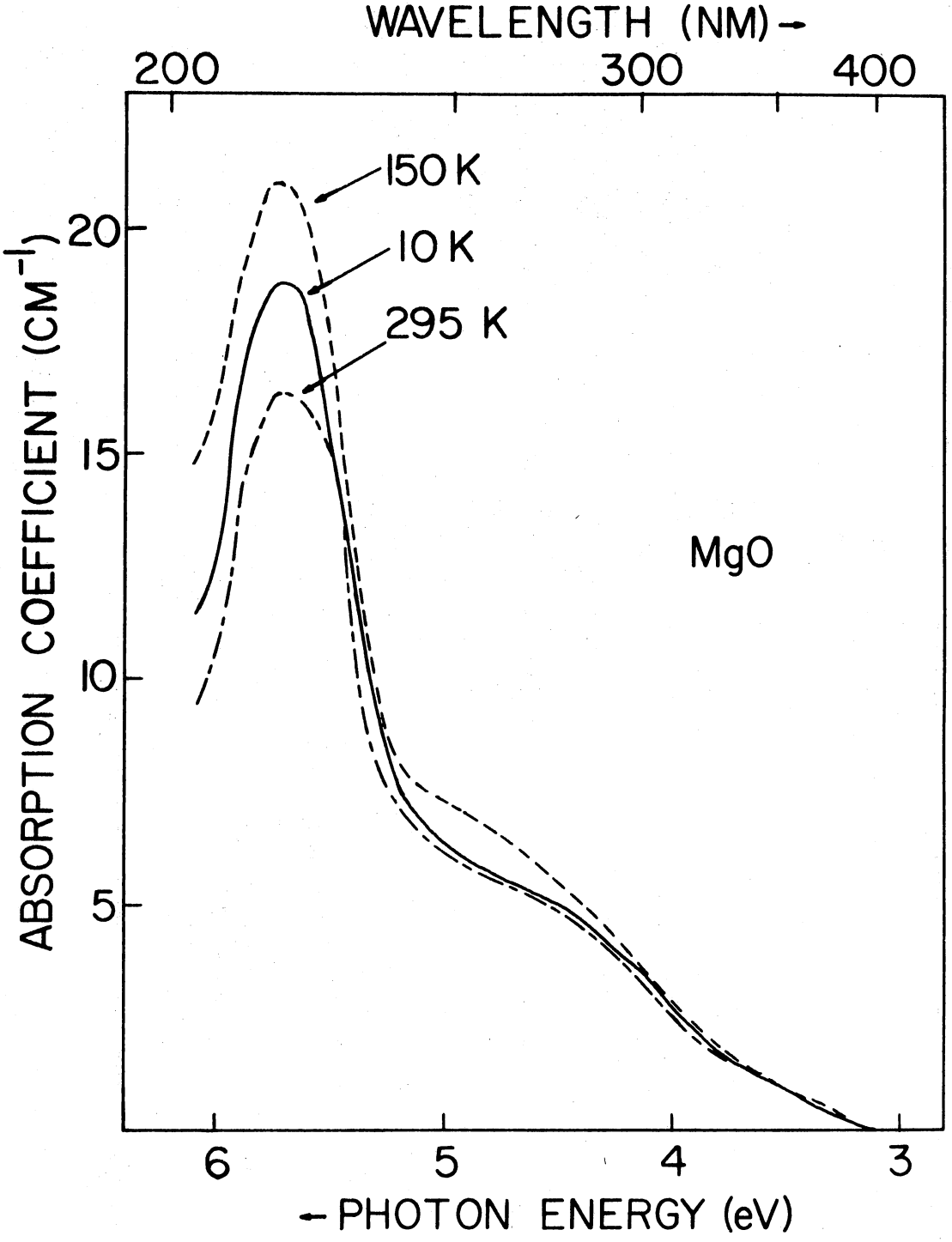

Figure 6. Absorption Spectra for Deformed MgO

A luminescence emission band in deformed MgO has been reported at 2.9 eV (440 nm) when excited by U.V. light (12). Figure 7 shows the emission intensity of the 2.9 eV band as a function of per cent deformation. Measurements were made on two samples, as indicated by circles and triangles in the figure. The emission was excited at room temperature with light of wavelength 238 nm from a 100W Hg lamp. Error was due mainly to inaccuracy in duplicating the exact position of the sample in the holder between successive deformations and to changes in the surface condition of the sample which altered the amount of light scattered. We see that the intensity increases progressively with deformation which agrees with the results obtained for absorption. We note that some luminescence is present even before the samples were deformed. This luminescence is probably due to dislocation-induced defects produced by cleaving the crystal.

The excitation spectrum at room temperature of the 150W Xe lamp in deformed MgO is shown in Figure 8. The excitation spectrum shows excitation peaks at 222 nm and 238 nm. The 238 nm peak decreases to nearly zero as temperature decreases. The 222 nm peak remains constant with temperature.

Annealing of the defects responsible for the absorption and emission was done by heating the samples in a furnace in air at the desired temperature for periods of ten minutes and then cooling the samples quickly by placing them on an aluminum block. Annealing data is presented in Figure 9. Data was taken on two samples as indicated by circles and triangles in the figure. Defects responsible for the absorption begin to anneal out at about 750 K and are almost completely gone at 1200 K. This result is in close agreement with annealing data

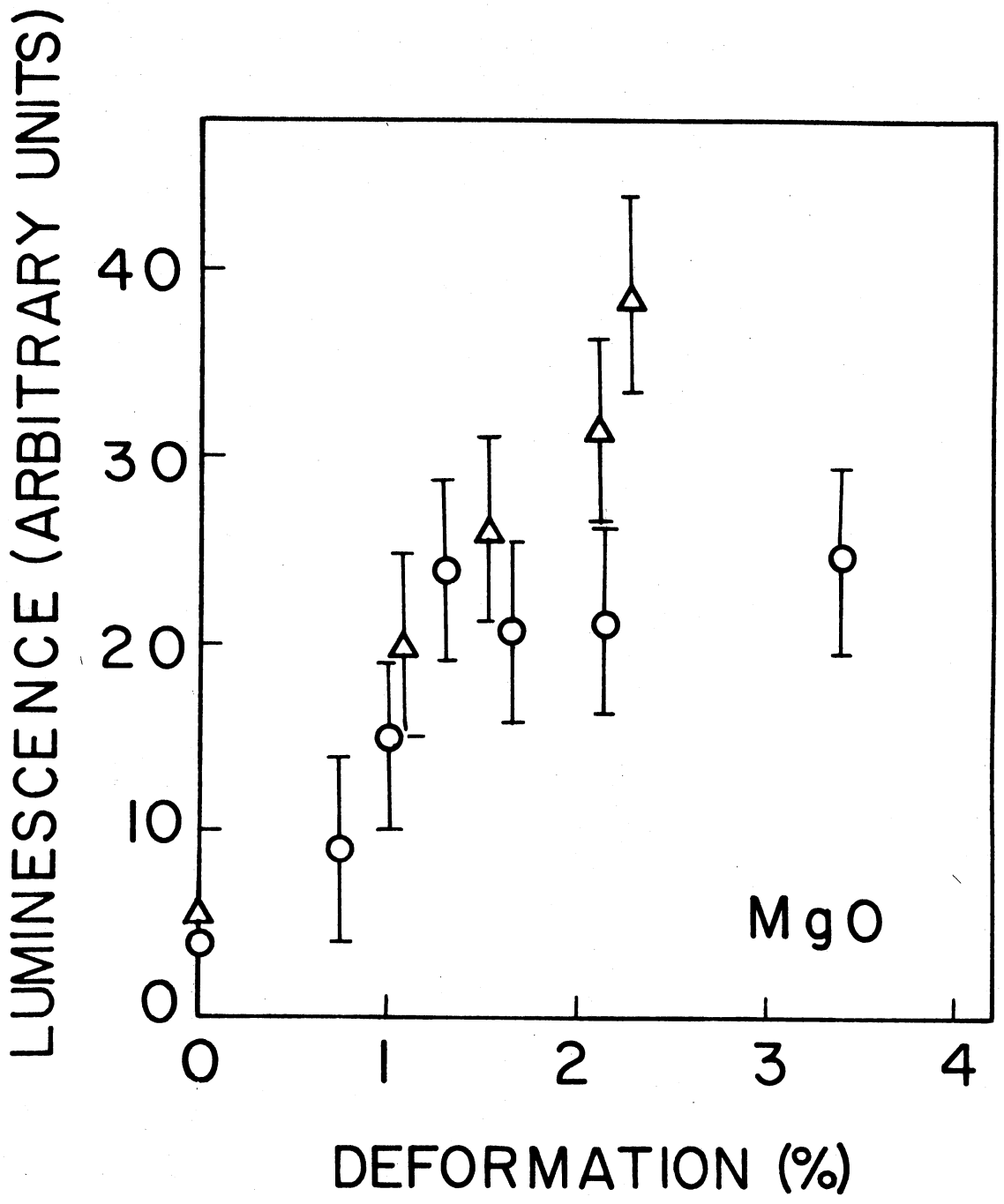

Figure 7. Intensity of 440 nm Luminescence Band as a Function of % Deformation in MgO

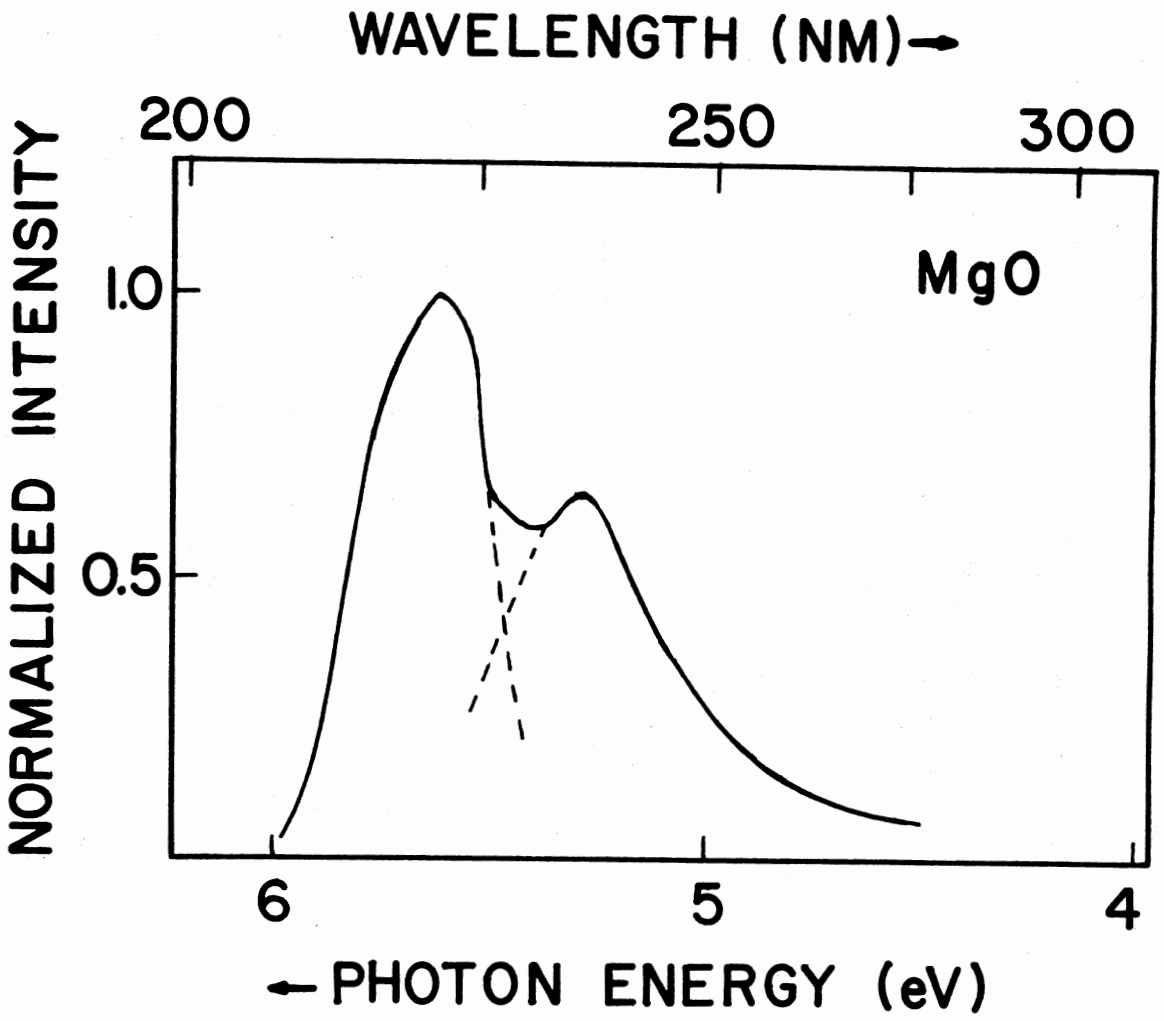

Figure 8. Excitation Spectrum at Room Temperature of 150W Xe Lamp in Deformed MgO

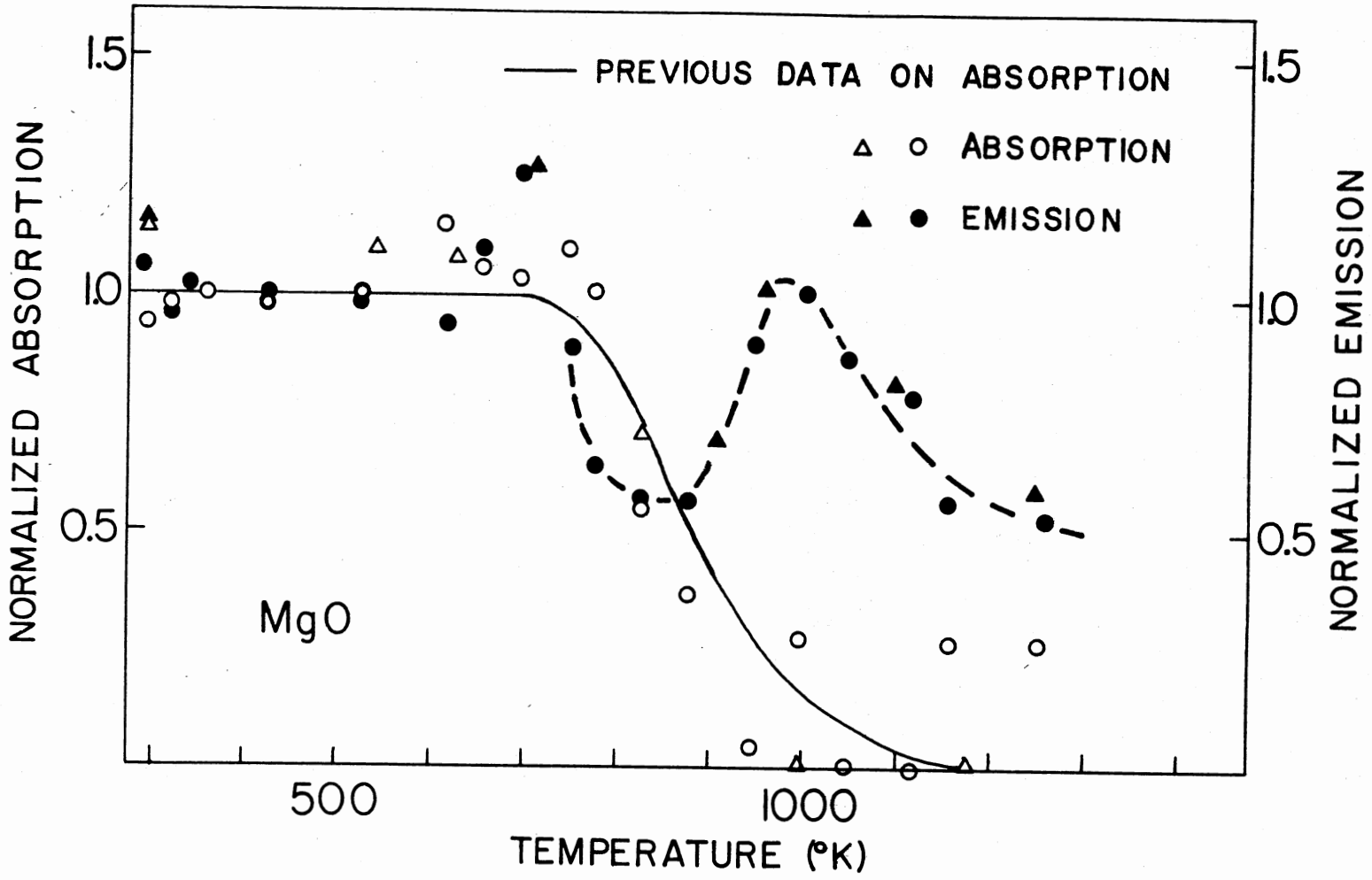

Figure 9. Annealing of 215 nm Absorption Band and 440 nm Emission Band in Deformed MgO. Results of a previous experiment by Sibley, et al. (19) are shown for purpose of comparison

from a previous experiment by Sibley, et al. (19). The emission begins to anneal at approximately the same temperature as does the absorption. However, at about 800 K the emission reaches its lowest intensity of 50% of its initial value and begins to increase. At 1000 K the emission reaches a peak equal to its initial intensity. This behavior would indicate that more than one type of defect is responsible for the emission, with an energy transfer process taking place.

The temperature dependence of the 215 nm absorption band and the 440 nm emission band is shown in Figure 10. The sample used in this experiment had a length to thickness ratio of 4.3 and was deformed 1.2%. The emission was excited by light of wavelength 220 nm from a 150W Xe lamp. The decrease of emission intensity below 220 K is another indication of energy transfer processes, perhaps with different types of defects being responsible for emission and absorption.

Thermoluminescence data was taken to determine if the blue thermoluminescence observed in deformed MgO is due to deformation-induced defects or to changes in valence states of iron impurity ions as has been reported previously (19,23). Thermoluminescence measurements were carried out on samples which had been gamma-irradiated for periods of 30 minutes immediately prior to each thermoluminescence run. The glow curve of the thermoluminescence peaked at about 85^{o}C. The spectrum of the thermoluminescence showed the glow peak to be composed of a broad band at 440 nm (blue) and a somewhat narrower band at 750 nm (red). The red band has been attributed to chromium impurity ions (19,23), so the intensity of the red band is constant regardless of the amount the sample is deformed. For this reason, the intensity of the blue band could be normalized to the intensity of the red band. The results of

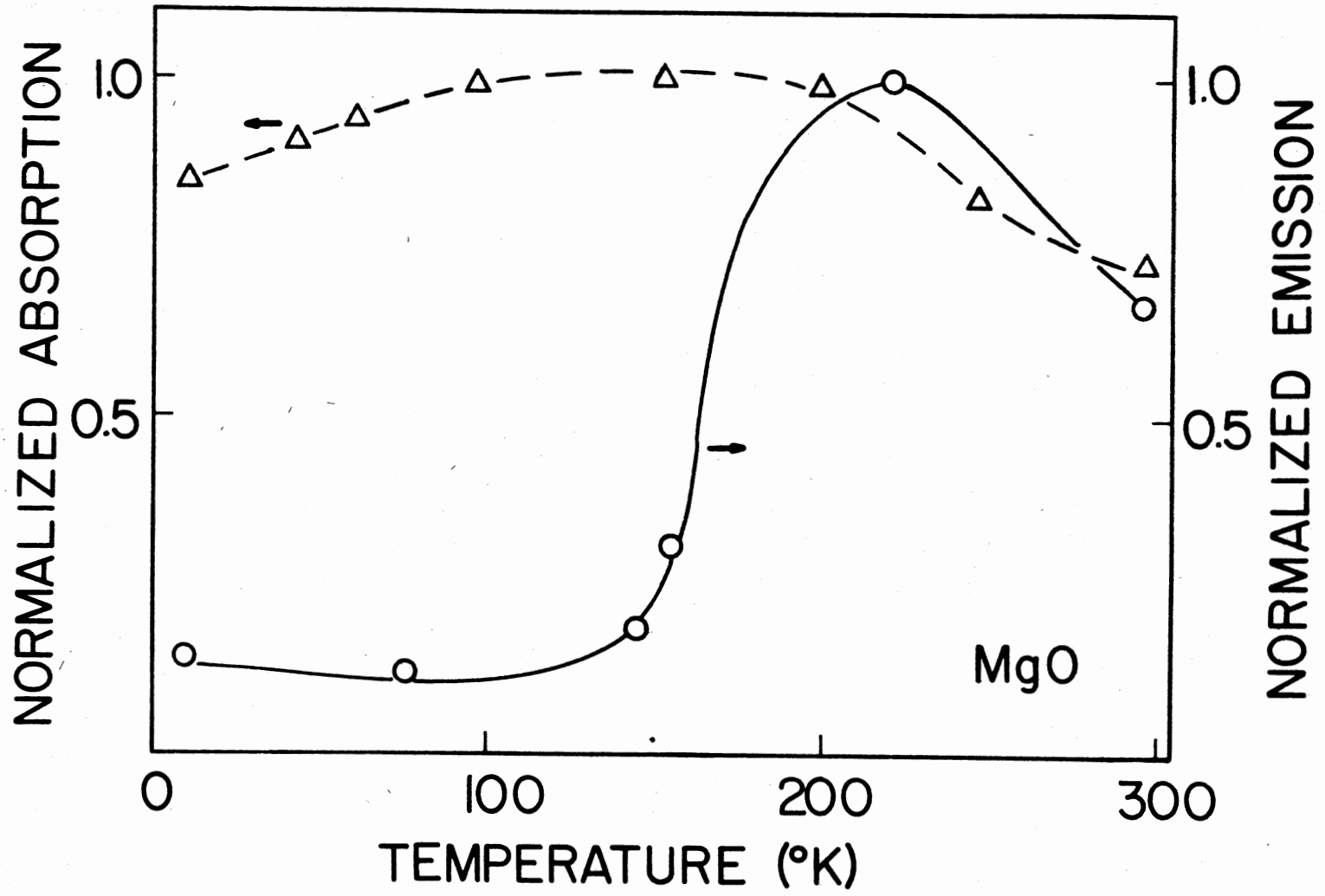

Figure 10. Temperature Dependence of the 215 nm Absorption Band and the 440 nm Emission Band in Deformed MgO

the study of the thermoluminescence is shown in Figure 11. The intensity of the red band would be a constant at a value of 13. We see that the intensity of the blue band increases linearly with deformation above 1.5%. What happens to the thermoluminescence below 1.5% is not clear because cleaving the sample deforms it somewhat and produces some dislocation type defects. Several of the samples were annealed after making thermoluminescence runs on them. Annealing was done by heating the samples slowly to a temperature of about 970^{o}C, holding them at this temperature for 30 minutes, and then allowing them to cool slowly to room temperature. The samples were then re-irradiated for 30 minutes and thermoluminescence runs were repeated. We expected to see the blue thermoluminescence decrease to the level of the as-cleaved sample, however we detected very little change in the thermoluminescence compared to the results from the as-deformed sample.

The spectrum of the blue thermoluminescence compared to that of the excited luminescence is shown in Figure 12. The two bandshapes are very similar. This fact, together with the linear dependence of thermoluminescence intensity on deformation leads us to suggest that the blue thermoluminescence is primarily a result of deformation-induced defects rather than only valence changes of iron impurity ions.

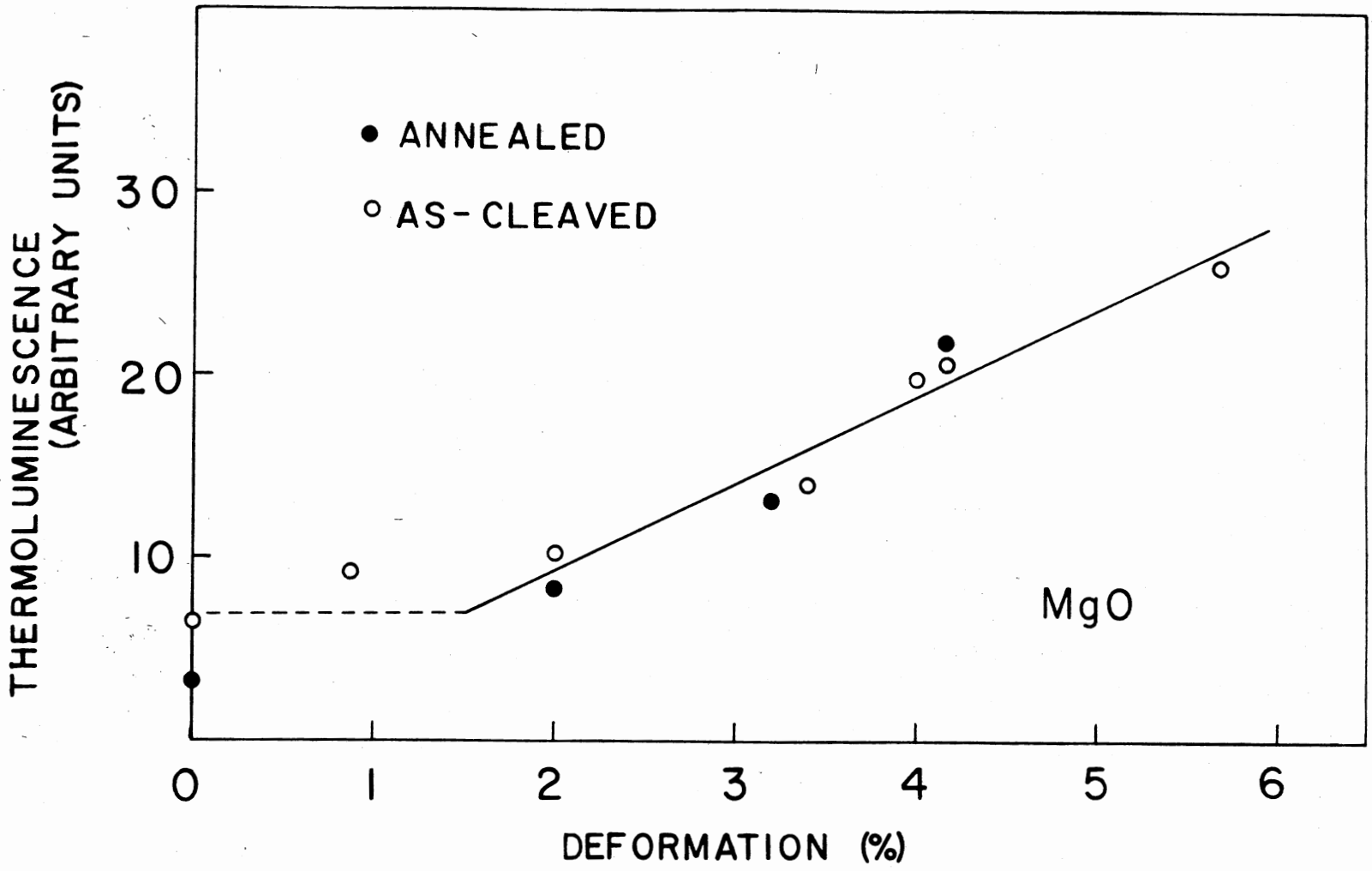

Figure 11. Thermoluminescence at 440 nm as a Function of % Deformation in MgO

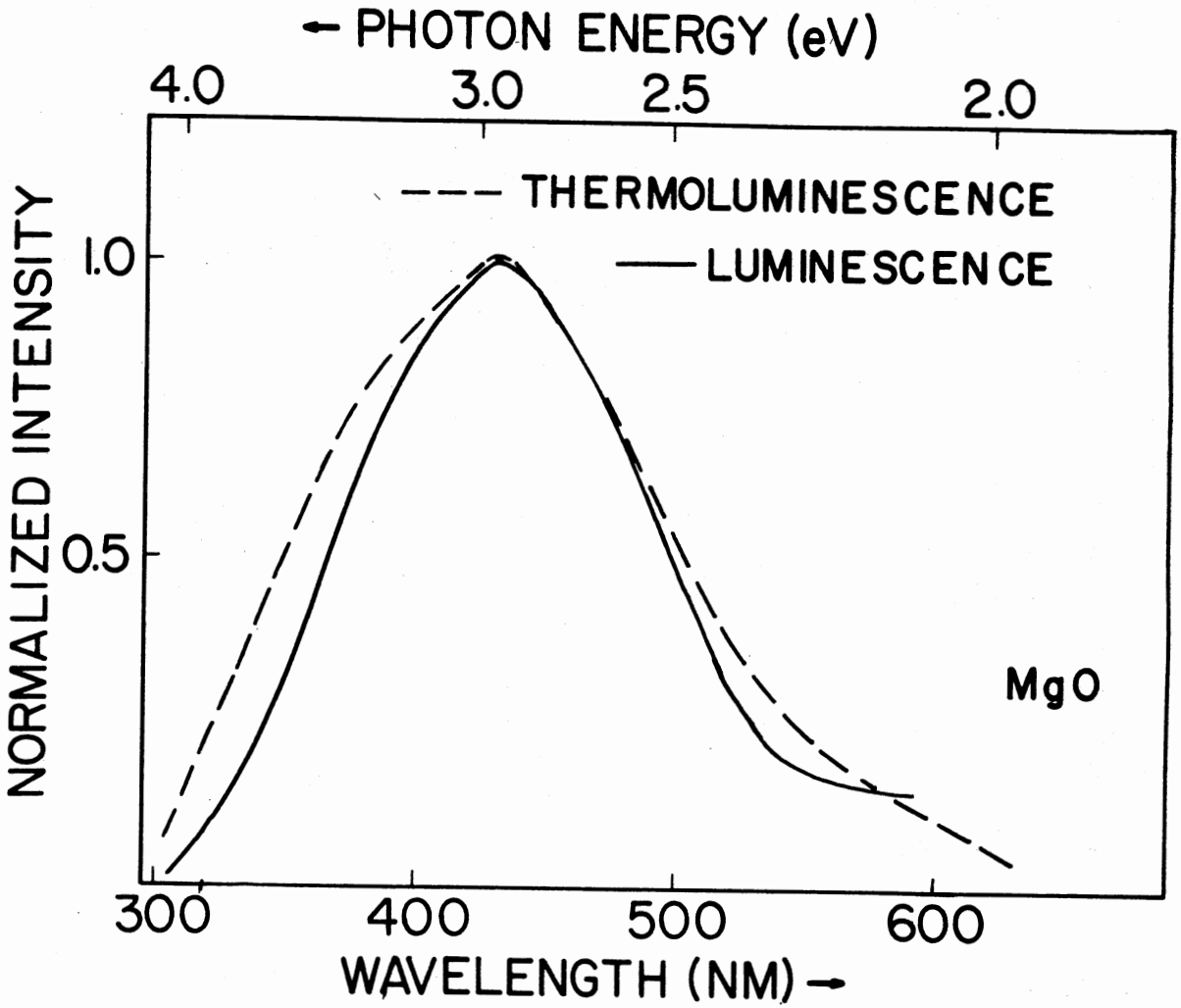

Figure 12. Thermoluminescence and Excited Luminescence Spectra for Deformed MgO

CHAPTER V

SUMMARY AND SUGGESTIONS FOR FUTURE STUDY

Absorption, luminescence and thermoluminescence studies were made on MgO samples which had been deformed by compression. The height of the 215 nm (5.7 eV) absorption band was found to increase linearly with strain. There appears to be a shape factor which contributes to the absorption. Long, thin samples have a higher absorption coefficient per % deformation than do short, thick ones. The difference is probably due to vacancy pairs being produced in long, thin samples while vacancy clusters are produced in short, thick samples.

Luminescence at 440 nm (2.9 eV) is produced in deformed MgO by exciting the sample with U.V. light. The intensity of the 440 nm emission band also increases with increasing deformation. The luminescence appears to be due to more than one type of defect as indicated by annealing and temperature dependence studies.

The intensity of the thermoluminescence band at 440 nm is also a linear function of deformation. The blue thermoluminescence appears to be due primarily to deformation rather than to impurity ions.

Some suggestions for future study are:

(1) Deform MgO at liquid nitrogen temperature and observe the effect of low temperature on the stress vs. strain curve. This experiment would help to determine if strain hardening is due to cross-slip or to the Orowan mechanism (27).

(2) Deform MgO at high (300°C) and low (77 K) temperatures to see if the absorption coefficient, α_{215}, vs. % deformation curve is temperature dependent.

(3) Deform MgO samples with different crosshead speeds on the Instron to determine the effect of different strain rates.

(4) Examine more closely the 302 nm band in deformed MgO to determine if the 215 nm and 302 nm bands are related (21).

(5) Once a firm background of knowledge about the optical properties of deformed pure MgO crystals has been established, one could then perform similar experiments on MgO doped with Mn or Co and MgO additively colored with Mg.

SELECTED BIBLIOGRAPHY

(1) Kelley, A. and G. W. Groves, Crystallography and Crystal Defects, (Longmans, London, 1970).

(2) Seitz, F., Advances in Physics, 1, 43 (1952).

(3) Davidge, R. W., C. E. Silverstone, and P. L. Pratt, Phil. Mag., 44, 985 (1959).

(4) Hull, D., Introduction to Dislocations (Pergamon Press, New York, 1965).

(5) Gilman, J. J., and W. G. Johnson, Solid State Physics, 13, 147 (1962).

(6) Amelinckx, S., Nuovo Cimento Supp., 7, 569 (1958).

(7) Hedges, J. M., and J. W. Mitchell, Phil. Mag., 44, 223 (1953).

(8) Hirsch, P. B., J. Inst. Metals, 87, 406 (1959).

(9) Brandon, D. G., and M. Wald, Phil. Mag., 6, 1035 (1961).

(10) Wertz, J. E., Defects and Transport in Oxides, Ed. by Seltzer and Jaffee (Plenum Press, New York, 1974).

(11) Henderson, B., and A. K. Garrison, Advances in Physics, 22, 423 (1973).

(12) Chen, Y., M. M. Abraham, T. J. Turner, and C. M. Nelson, Phil. Mag., 32, 99 (1975).

(13) Miller, R. L., T. A. Coultas et al., Trans. Am. Nucl. Soc., 17, 39 (1973).

(14) Gilman, J. J., and W. G. Johnson, Dislocations and Mechanical Properties of Crystals, Ed. by Fisher et al. (John Wiley and Sons, Inc., 1957).

(15) Kelley, A., and G. K. Williamson, Phil. Mag., 5, 991 (1960).

(16) Cass, R. T., and J. Washburn, Proc. Brit. Ceram. Soc., 6, 239 (1966).

(17) Wertz, J. E., P. Auzins, R. A. Weeks, and R. H. Silsbee, Phys. Rev., 107, 1535 (1957).

(18) Klein, M. J., and W. B. Gager, J. Appl. Phys. 37, 4112 (1966).

(19) Sibley, W. A., J. L. Kolopus, and W. C. Mallard, Phys. Stat. Sol., 31, 223 (1969).

(20) Turner, T. J., N. W. Isenhower, and P. K. Tse, Sol. State Comm. 7, 1661 (1969).

(21) Turner, T. J., C. Murphy, and T. Schultheiss, Phys. Stat. Sol., 58, 843 (1973).

(22) Vellednilskaya, M. A., V. N. Rozahanskii, et al., Phys. Stat. Sol., (a), 32, 123 (1975).

(23) Takeuchi, N., K. Inabe, and H. Nanto, Sol. State Comm., 17, 1267 (1975).

(24) Cottrell, A. H., Dislocations and Plastic Flow in Crystals (Oxford University Press, London, 1953).

(25) Frenkel, J., Zeit. Phys., 37, 572 (1926).

(26) Mackenzie, J. K., Thesis (University of Bristol, 1949).

(27) Kovacs, I., and L. Zsoldos, Dislocations and Plastic Deformation (Pergamon Press, Oxford, 1973).

(28) Taylor, G. I., Proc. Roy. Soc. London, A145, 362 (1934).

(29) Gilman, J. J., Progress in Ceramic Science, 1, 146 (1961).

(30) Gilman, J. J., and W. G. Johnson, J. Appl. Phys., 30, 129 (1959).

(31) Fleischer, R. L., Acta. Met., 10, 835 (1962).

(32) Akimoto, K., and W. A. Sibley, J. Appl. Phys., 34, 1767 (1962).

(33) Gilman, J. J., and W. G. Johnson, J. Appl. Phys., 31, 687 (1960).

(34) Gilman, J. J., J. Appl. Phys., 33, 2703 (1962).

(35) Johnson, W. G., J. Appl. Phys., 33, 2716 (1962).

VITA

Ricky Dan Newton

Candidate for the Degree of

Master of Science

Thesis: OPTICAL PROPERTIES OF DEFORMATION INDUCED DEFECTS IN MgO SINGLE CRYSTALS

Major Field: Physics

Biographical:

Personal: Born in Ada, Oklahoma, June 10, 1952, the son of Ran and Arvilla Newton.

Education: Grduated from Latta High School in Ada, Oklahoma, in May, 1970; received Bachelor of Science degree in Physics and Mathematics from East Central Oklahoma State University in Ada, Oklahoma in May, 1974; completed requirements for Master of Science degree at Oklahoma State University in December, 1976.